International Microbiology
https://doi.org/10.1007/s10123-024-00582-y

RESEARCH

Functional redundancy and niche specialization in honeybee and *Varroa* microbiomes

Štefánia Skičková[1] · Myriam Kratou[2] · Karolína Svobodová[3] · Apolline Maitre[4,5,6] · Lianet Abuin-Denis[4,7] · Alejandra Wu-Chuang[4] · Dasiel Obregón[8] · Mourad Ben Said[2,9] · Viktória Majláthová[1] · Alena Krejčí[3,10] · Alejandro Cabezas-Cruz[4]

Received: 19 June 2024 / Revised: 7 August 2024 / Accepted: 13 August 2024

Abstract
The honeybee (*Apis mellifera*) is a key pollinator critical to global agriculture, facing threats from various stressors, including the ectoparasitic *Varroa* mite (*Varroa destructor*). Previous studies have identified shared bacteria between *Varroa* mites and honeybees, yet it remains unclear if these bacteria assemble similarly in both species. This study builds on existing knowledge by investigating co-occurrence patterns in the microbiomes of both *Varroa* mites and honeybees, shedding light on potential interactions. Leveraging 16S rRNA datasets, we conducted co-occurrence network analyses, explored Core Association Networks (CAN) and assess network robustness. Comparative network analyses revealed structural differences between honeybee and mite microbiomes, along with shared core features and microbial motifs. The mite network exhibited lower robustness, suggesting less resistance to taxa extension compared to honeybees. Furthermore, analyses of predicted functional profiling and taxa contribution revealed that common central pathways in the metabolic networks have different taxa contributing to *Varroa* mites and honeybee microbiomes. The results show that while both microbial systems exhibit functional redundancy, in which different taxa contribute to the functional stability and resilience of the ecosystem, there is evidence for niche specialization resulting in unique contributions to specific pathways in each part of this host-parasite system. The specificity of taxa contribution to key pathways offers targeted approaches to *Varroa* microbiome management and preserving honeybee microbiome. Our findings provide valuable insights into microbial interactions, aiding farmers and beekeepers in maintaining healthy and resilient bee colonies amid increasing *Varroa* mite infestations.

Keywords *Apis mellifera* · *Varroa destructor* · Microbiomes · Community assembly · Networks

✉ Štefánia Skičková
stefania.skickova@student.upjs.sk

✉ Alejandro Cabezas-Cruz
alejandro.cabezas@vet-alfort.fr

[1] Pavol Jozef Šafárik University in Košice, Faculty of Science, Institute of Biology and Ecology, Department of Animal Physiology, Košice 04181, Slovakia

[2] Laboratory of Microbiology, National School of Veterinary Medicine of Sidi Thabet, University of Manouba, 2010 Manouba, Tunisia

[3] University of South Bohemia, Faculty of Science, České Budějovice 37005, Czech Republic

[4] ANSES, INRAE, École Nationale Vétérinaire d'Alfort, UMR BIPAR, Laboratoire de Santé Animale, 94700 Maisons-Alfort, France

[5] INRAE, UR 0045 Laboratoire de Recherches Sur Le Développement de L'Elevage (SELMET-LRDE), 20250 Corte, France

[6] EA 7310, Laboratoire de Virologie, Université de Corse, 20250 Corte, France

[7] Animal Biotechnology Department, Center for Genetic Engineering and Biotechnology, Avenue 31 Between 158 and 190, P.O. Box 6162, 10600 Havana, Cuba

[8] School of Environmental Sciences, University of Guelph, Guelph, ON N1G 2W1, Canada

[9] Department of Basic Sciences, Higher Institute of Biotechnology of Sidi Thabet, University of Manouba, 2010 Manouba, Tunisia

[10] Czech Academy of Sciences, Biology Centre, Institute of Entomology, České Budějovice 37005, Czech Republic

Published online: 22 August 2024

Introduction

Varroa destructor (Parasitifiormes: Varroidae) is an ectoparasitic mite that infests western honeybees of *Apis mellifera* (Hymenoptera: Apidae) (Rosenkranz et al. 2010). *Varroa* is spread in all regions inhabited by *A. mellifera* colonies, except some locations such as remote islands (e.g., Seychelles, Comoros archipelagoes) as well as the extreme northern regions (Traynor et al. 2020). Historically, *Varroa* mite was believed to feed only on honeybee hemolymph. However, recent evidences indicate that while hemolymph is a major dietary component for *Varroa* mites during the reproductive phase when feeding on honeybee larvae (Han et al. 2024), phoretic mites feeding on adult honeybees acquire predominantly fat bodies (Ramsey et al. 2019; Han et al. 2024). The *Varroa* mite infestation on honeybee colonies weakens the host, attenuates the immune response (Kuster et al. 2014), reduces the ability to navigate (Ruano et al. 1991), prolongs the absence from the colony, and lowers the return rate to the hive (Krajl & Fuchs, 2006). Moreover, *Varroa* mites also act as vectors of several pathogenic viruses (Chen et al. 2004; Di Prisco et al. 2011; Piou et al. 2022; Tantillo et al. 2015) and bacteria (Kanbar and Engels 2003). For instance, *Varroa* mites facilitate the transmission of pathogenic bacteria such as *Serratia marcescens* (Gliński & Jarosz 1992) causing mortality of honeybees if applied to hemocoel (Raymann et al. 2018). The small punctures of *Varroa* mites to the pupal integument of honeybees induce wound formation where the microbial infection tends to spread (Kanbar and Engels 2003). Pathogens as well as other bacteria carry an ecological importance (Fischhoff et al. 2020) and pose a growing concern causing economic losses to beekeepers worldwide (Hristov et al. 2020).

Despite the increasing number of *Varroa* mite infestations, to the best of our knowledge, only four studies dealing with *Varroa* mite microbiome have been conducted to date—from Czechia (Hubert et al. 2016), Italy (Sandionigi et al. 2015), Thailand (Pakwan et al. 2018), and USA (Huang & Evans 2024). While these studies primarily focus on alpha and beta diversity description, only Huang and Evans (2024) analyzed the functional profile of *Varroa* mite´s microbiome and none of them have delved into the bacterial co-occurrence networks. Among them, only two experiments conducted in Czechia (Hubert et al. 2016) and Italy (Sandionigi et al. 2015), have compared the honeybee and *Varroa* mite microbiomes. Particularly, Hubert et al. (2016) examined the microbiota of honeybee *A. mellifera* and *Varroa* mites. Analyzing specimens from 26 colonies in Czechia, they found significant differences in microbiota diversity, with *Varroa* mites having a lower diversity. *Diplorickettsia*, a specific symbiont, was identified in *Varroa* mites, while certain bacterial taxa were more abundant in *Varroa* than in honeybees. The study supported the concept of bacterial transfer between the two populations, emphasizing distinct proportional representations in their microbiomes. The findings contribute to understanding the intricate dynamics of microbial interactions within the honeybee-*Varroa* system and highlight potential implications for honeybee health.

Analyzing microbial co-occurrence networks proves to be a valuable tool for investigating the structure and dynamics of microbial communities (Faust and Raes 2012; Layeghifard et al. 2017). By utilizing abundance data derived from high-throughput sequencing technologies, meaningful co-occurrence patterns between microbial taxa can be identified and visually represented as networks (Faust and Raes 2012). In these microbial networks, nodes and links symbolize bacterial taxa and their respective co-occurrences (Röttjers and Faust 2018). In addition, the study of emergent properties, such as robustness and connectivity, helps elucidate the behavior of complex systems like the bacterial microbiota. These properties would remain unnoticed if only isolated portions of the network were examined (Aderem 2005; Röttjers and Faust 2018). Networks have proven insightful in analyzing the honeybee microbiome and exploring *Varroa*-honeybees-virus interactions. Particularly, Svobodová et al. (2023) investigated the impact of *V. destructor* and associated viruses on honeybee gut microbiota, focusing on *Varroa*-susceptible and *Varroa*-surviving honeybees from Gotland. Employing a network approach with viral and bacterial nodes, they found distinct microbiota differences between the two honeybee populations. Four viruses were tightly linked to bacterial nodes in *Varroa*-susceptible honeybees, while *Varroa*-surviving honeybees exhibited less complex networks with fewer viral associations. In silico removal of viral nodes disrupted microbial networks and reduced robustness in *Varroa*-susceptible honeybees. The study highlights the importance of a network approach in understanding virus-bacterium interactions and their role in honeybee resistance, providing insights for controlling viral infections. Beyond unraveling microbial community assembly patterns and robustness, 16S rRNA data can be leveraged to predict metabolic function by aligning taxonomic information with metabolic reference databases (Douglas et al. 2020; Hou et al. 2021).

Moreover, Hubert et al. (2017) found significant changes in honeybee bacteriome after *Varroa* mite infestation while it was considered a more important factor than *Nosema* fungal pathogens (*Nosema ceranae* and *Nosema apis*) as well as trypanosome *Lotmaria passim*. The high level of varroosis has an impact on the bacterial composition as the immune system of honeybees is not fully capable of resisting the *Varroa* mite infestation.

Here, we used a network inference approach to analyze 16S rRNA metabarcoding data obtained from Hubert et al. (2016) and further characterized the microbial community

assembly and predicted functional profiles of *A. mellifera* and *V. destructor* microbiomes. While Hubert et al. (2016) identified shared bacteria, our inquiry delved into whether the co-occurrence of these bacteria persisted within the microbial communities of both *Varroa* mites and honeybees. Our hypothesis posited that host specificity might influence interactions between microbes or between microbes and hosts, thereby resulting in variations in overall community assembly and function that extend beyond taxonomic distinctions alone. Our investigation revealed divergent contributions from different taxa in core metabolic pathways of the metabolic networks within *Varroa* mites and honeybee microbiomes. The findings imply that niche specialization among bacterial taxa leads to distinct contributions to specific pathways, ultimately causing the observed differences in representation between *Varroa* mites and honeybee microbiomes. Targeting *Varroa*-specific bacterial taxa that contribute to central and core metabolic pathways provides a promising approach for developing interventions to control this pest.

Methods

Original 16S rRNA dataset

In the present study, we used available 16S rRNA amplicon sequence datasets. In the original study, Hubert et al. (2016) compared the microbial diversity of *A. mellifera* honeybees and *V. destructor* mites within the hives. The samples were collected from seven apiaries from the Czech Republic and all of them were linked into 26 pairs of honeybees and mites. Both samples were pooled—honeybee samples consisted of 10 worker honeybees while the number of mite samples ranged from 10 to 50 female individuals. A 16S rRNA gene fragment was PCR amplified by barcoded primers 27Fmod/ill519Rmod and sequenced in Illumina TruSeq. Generated data were deposited in the National Center for Biotechnology Information (NCBI) GenBank under the SRA number SRP067076.

Analysis of 16S rRNA amplicon sequences

For the recent study, the amplicon sequence variants (ASV) were downloaded in Quantitative Insights Into Microbial Ecology (QIIME2) 2023.7 environment (Bolyen et al. 2019) using the q-fondue script (Ziemski et al. 2022). Two samples (one of *Apis* honeybee and one of *Varroa* mite) were discarded from this analysis due to the inaccuracies in the accession number. Except that there were also two other samples with misleading information provided meaning that the samples *A. mellifera* female and *V. destructor* worker were analyzed; however, these data were the most probably exchanged. Afterward, these data were demultiplexed, denoised, quality trimmed, merged, chimera removed, and filtered in the DADA2 software (Callahan et al. 2016) and implemented in the QIIME2 environment (Bolyen et al. 2019). The representative sequences were annotated using the Bayes taxonomic classifier (Bokulich et al. 2018) based on the 16S rRNA SILVA database (Yarza et al. 2014). The resulting taxonomic table was subsequently used in the further network analysis and pathway prediction.

Bacterial co-occurrence networks

Co-occurrence network analysis was performed using the sparse correlations for computational data (SparCC) method (Friedman and Alm 2012), in RStudio (RStudio Team 2020). Taxonomic data tables were used to calculate the correlation matrix. Correlation coefficients with SparCC ≥ 0.3 or ≤ -0.3 (weak) and SparCC ≥ 0.5 or ≤ -0.5 (strong) were selected. Network visualization and calculation of topological features and taxa connectedness (i.e., number of nodes and edges, modularity, network diameter, average degree, weighted degree, clustering coefficient, and centrality metrics) were performed using the software Gephi 0.9.2 (Bastian et al. 2009).

Network robustness analysis

We assessed the robustness of microbial co-occurrence networks by examining the effects of node removal or addition on network connectivity. To assess this, we simulated the loss in connectivity resulting from removing a fraction of nodes in the network with more connections (SparCC ≥ 0.3 or ≤ -0.3), employing both random and directed attacks. For the directed attack, we utilized three strategies: betweenness centrality, degree centrality, and cascading. In the betweenness centrality approach, nodes with the highest betweenness centrality values were sequentially removed. In the degree centrality approach, nodes with the highest degree centrality values were prioritized for removal. In the cascading approach, nodes with the highest betweenness centrality values were initially removed, and betweenness centrality was recalculated after each node removal. To conduct the network robustness analysis, we employed the network strengths and weaknesses analysis (NetSwan) package (Lhomme 2015) in RStudio (RStudio Team 2020).

Additionally, node addition analysis was conducted also using RStudio (RStudio Team 2020) based on the method outlined by Freitas et al. (2021). In this analysis, new nodes were randomly connected to the existing network and assessed by the largest connected component (LCC) and the average path length (APL). To enhance the precision of the network's robustness assessment, we repeated the simulation with different sets of nodes, introducing 100, 300, 500,

700, and 1000 nodes. The resulting values were visualized using GraphPad Prism 9.0.2 (GraphPad Software Inc., San Diego, CA, USA).

Comparative network analysis

The network similarity was compared with the Network Construction and Comparison for Microbiome data (NetCoMi) package (Peschel et al. 2021), in RStudio (RStudio Team 2020). The analysis was performed for the network with more connections with SparCC ≥ 0.3 or ≤ -3. The Jaccard index measuring various network properties (e.g., degree, betweenness, closeness, eigenvector, and hub taxa) expresses the similarity of several of the most central nodes. The Jaccard index measures the level of node similarity and ranges from 0 (totally different) to 1 (unique). The *p*-values, either $P(J \leq j)$ or $P(J \geq j)$, correspond to "less than or equal" and "higher than or equal," and represent the likelihood of the Jaccard index to the expected Jaccard value.

The CAN analysis function was used to evaluate common nodes and edges between two different networks. The core of the *Varroa* and honeybee networks was determined at two different co-occurrence correlations (SparCC ≥ 0.3 or ≤ -0.3 and SparCC ≥ 0.5 or ≤ -0.5) using the Anuran toolbox (Röttjers et al. 2021) with default parameters. This analysis was conducted in the Anaconda Python environment (Anaconda Software Distribution 2023).

Functional profile prediction

To predict the microbial functional traits, specifically the enzymatic pathways, the PICRUSt2 (Phylogenetic Investigation of Communities by Reconstruction of Unobserved States) (Douglas et al. 2020) in QIIME2 environment (Bolyen et al. 2019) was applied. Several gene catalogs (e.g., Kyoto Encyclopedia of Genes and Genomes (KEGG), Orthologs (KO), Enzyme Classification numbers (EC), and Cluster of Orthologous Genes (COGs)) (Kanehisa 2000) and MetaCyc database (Caspi et al. 2018) were employed to interfere with major pathway categories and mapping. Following the output table, various analyses were performed (e.g., alpha and beta diversity, DESeq2, co-occurrence network, CAN, Venn diagram, and Sankey) to provide proper and considerable statistical analysis. Alpha diversity was explored by observed features (DeSantis et al. 2006) and Pielou's evenness (Pielou 1966) using a Kruskal–Wallis statistical test ($p < 0.05$) estimated in the QIIME2 plugin. Beta diversity (Su 2021) was carried out by PCoA (Principal Coordinates Analysis) plot using the Bray–Curtis distance matrix (Hammer et al. 2001) and PERMANOVA test ($p < 0.05$) also in QIIME2 (Bolyen et al. 2019) and ANOVA test ($p < 0.05$) with Betadisper script (Oksanen et al. 2022) in RStudio (RStudio Team 2020). The differences in pathway frequency were measured by the Wald test with Benjamini–Hochberg correction ($p < 0.05$) in order to calculate the false discovery rate. The analysis was performed by the DESeq2 package (Love et al. 2014) in RStudio (RStudio Team 2020) resulting in a volcano plot. The co-occurrence networks of functional profiles were performed the same way as for bacterial networks using the SparCC package (Friedman and Alm 2012) and Gephi software 0.9.2. The threshold value applied for these networks was SparCC ≥ 0.75 or ≤ -0.75. Also, CAN analysis was conducted following the same methodology as for taxonomic data. The quantification of unique and shared metabolic pathways was measured by a Venn diagram using the online tool available on the webpage https://bioinformatics.psb.ugent.be/webtools/Venn/.

Correlation analysis

The topological features (i.e., degree, eigenvector, and betweenness centrality) of taxa and pathways present in the networks of both, *A. mellifera* and *V. destructor*, were put into the correlation using GraphPad Prism 9.0.2 (GraphPad Software Inc., San Diego, CA, USA). For taxa correlation analysis, the data from the network with the threshold value of SparCC ≥ 0.3 or ≤ -0.3 were selected. The statistical significance was calculated by Spearman statistical analysis chosen according to Shapiro–Wilk and Anderson–Darling tests for normality and lognormality.

Connections between functional and taxonomic profiles

To investigate the links between functionality, five of the most central pathways were chosen from CAN analysis according to their degree, supported by eigenvector centrality. This analysis was performed using the scripts of network D3 (Allaire et al. 2017) and htmlwidgets (Vaidyanathan et al. 2023) in RStudio (RStudio Team 2020). The values of taxon relative function abundance higher than 100 were counted into consideration, included in the analysis, and displayed on the Sankey graph.

Clustering analysis of metagenome

The clustering analysis of metagenome (CLAM) (Chazdon et al. 2011) was performed using RStudio (RStudio Team 2020). This analysis categorized the taxa within honeybees and *Varroa* microbiomes into different groups based on their interactions with these specific hosts. These groups include specialists (organisms that have a narrow range of hosts or environmental conditions), generalists (organisms that can thrive in a wide range of conditions or with multiple hosts), or taxa that are too rare to be classified into these categories.

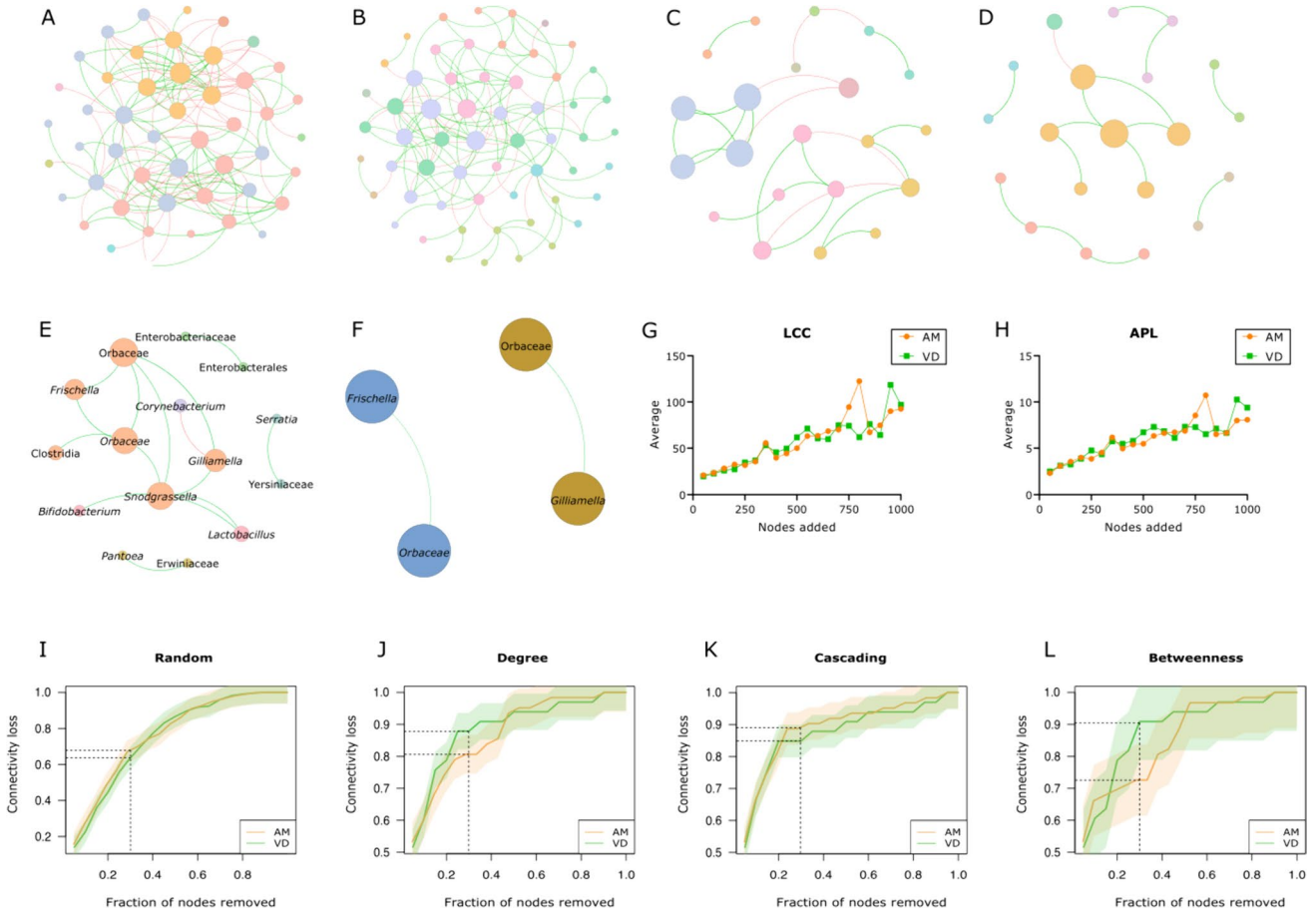

Fig. 1 Microbial network analysis. Microbial co-occurrence networks with different thresholds, namely *A. mellifera* SparCC ≥ 0.3 or ≤ −0.3 (**A**), *V. destructor* SparCC ≥ 0.3 or ≤ −0.3 (**B**), *A. mellifera* SparCC ≥ 0.5 or ≤ −0.5 (**C**), *V. destructor* SparCC ≥ 0.5 or ≤ −0.5 (**D**), CAN SparCC ≥ 0.3 or ≤ −0.3 (**E**), and CAN SparCC ≥ 0.5 or ≤ −0.5 (**F**). The Orbaceae family and genus are distinguished by normal and italics font, respectively. Nodes stand for bacterial taxa, and their size is proportional to eigenvector centrality. The node color is based on the modularity class; therefore, the nodes with the same color are part of the same cluster. Red and green edges represent negative and positive interactions, respectively. Only the nodes with at least one link are shown. Robustness comparison of sp *A. mellifera* and *V. destructor* networks. Node addition was measured by LCC (**G**) and APL (**H**). Node removal was evaluated by random (**I**), degree (**J**), cascading (**K**), and betweenness (**L**) methods. Orange and green colors represent *A. mellifera* and *V. destructor*, respectively

Graph edition

All graphs were edited by Inkscape 1.3.2 (Boston, MA, USA) software.

Results

Community assembly and network robustness in the *Varroa* and honeybee microbiomes

In examining the microbial interactions within the microbiomes of *Varroa* mites and honeybees, co-occurrence network analyses were conducted using two thresholds, SparCC ≥ 0.3 or ≤ −0.3, SparCC ≥ 0.5 or ≤ −0.5). At the lower threshold, the honeybee network (Fig. 1A) displayed a higher average degree, modularity, and number of edges compared to the *Varroa* network (Fig. 1B, Table 1) . . Conversely, for other metrics (Table 1), the mite's microbiome presented higher values. Upon applying the higher threshold for interactions, it was found that the network associated with the honeybee microbiome (Fig. 1C) exhibited higher values in various topological features, including connectivity and network complexity, indicating a wider range of interactions (Table 1). In contrast, the *Varroa* mite's network (Fig. 1D) showed a lower degree of these characteristics, with the exception of the average strength of connections (Table 1).

The Core Association Network (CAN) analysis highlighted shared core interactions between the two species' microbiomes. At the lower threshold (Fig. 1E), the network was more intricate, with 15 nodes and 14 edges, whereas the network at the higher threshold (Fig. 1F) was simpler with

Table 1 Topological features of taxonomic co-occurrence networks

Topological features	AM30[a]	VD30[b]	AM50[a]	VD50[b]
Average degree	6.68	4.586	2.19	1.5
Average weighted degree	0.331	0.945	0.685	0.707
Network diameter	5	7	6	4
Modularity	3.712	0.948	1.025	0.798
Average clustering coefficient	0.608	0.315	0.44	0.214
Nodes	50	58	21	20
Edges	167	133	23	15
Positives	91 (54.49%)	99 (74.44%)	17 (73.91%)	14 (93.33%)
Negatives	76 (45.51%)	34 (25.56%)	6 (26.09%)	1 (6.67%)

[a]*A. mellifera* (AM, networks at threshold of SparCC ≥ 0.3 or ≤ −0.3 (AM30) and SparCC ≥ 0.5 or ≤ −0.5 (AM50))

[b]*V. destructor* (VD, networks at threshold of SparCC ≥ 0.3 or ≤ −0.3 (VD30) and SparCC ≥ 0.5 or ≤ −0.5 (VD50))

Table 2 Topological features of Core Association Networks

Topological parameters	CAN30[a]	**CAN50[a]**
Average degree	1.867	1
Average weighted degree	0.785	0.654
Network diameter	4	1
Modularity	0.488	0.497
Average clustering coefficient	0.417	NaN
Nodes	15	4
Edges	14	2
Positives	13 (92.86%)	2 (100%)
Negatives	1 (7.14%)	0 (0%)

[a]Core association network (CAN). Networks at SparCC ≥ 0.3 or ≤ −0.3 (CAN30) and SparCC ≥ 0.5 or ≤ −0.5 and 0.5 (CAN 50)

four nodes and two edges (Table 2). This difference underscores the variability in microbial interaction complexity and connectivity across different analysis thresholds within the microbiomes of these species.

An important feature of networks is their ability to withstand perturbation by addition and/or removal of nodes. In our study, by modeling the addition of 1000 nodes to each network (SparCC ≥ 0.3 or ≤ −0.3) and observing the changes in two graph properties, the largest connected component (LCC) (Fig. 1G) and average path length (APL) (Fig. 1H), it was found that both properties increased with the addition of nodes. High LCC suggests that the microbiomes of both species are robust, with a high level of ecological interactions (e.g., nutrient cycling), while the high APL indicates a modular structure, where certain groups of species interact more closely within themselves than with the broader community.

When 30% of the nodes were randomly removed, both the honeybee and *Varroa* mite networks experienced a similar reduction in connectivity (Fig. 1I). However, when a targeted attack based on node degree was conducted, the honeybee network proved to be more resilient than the *Varroa* network (Fig. 1J). Conversely, during a cascading attack, where the removal of one node affects others, the *Varroa* network displayed greater robustness compared to the honeybee network (Fig. 1K). The most significant difference in resilience was seen during a targeted attack based on node betweenness. After removing 30% of the nodes in this manner, the *Varroa* network was found to be nearly 20% less resilient than the honeybee network (Fig. 1L).

Hierarchical structure of the Varroa and honeybee microbiomes

A comparative network analysis was conducted to identify differences in the microbiome connectivity of honeybees and *Varroa* mites. Visual inspections of the network for honeybees (Fig. 2A) and for *Varroa* mites (Fig. 2B) showed significant variations in connectivity patterns. The analysis of changes in connectivity revealed a predominant shift from positive to negative interactions and vice versa between the two networks (Fig. 2C).

Correlation analyses focusing on centrality measures of nodes present in both microbiomes were performed. It was found that the values of degree (Spearman $r = 0.41$, $p = 0.02$) (Fig. 3A) and eigenvector (Spearman $r = 0.50$, $p = 0.004$) (Fig. 3B) centrality were significantly correlated, suggesting that key species that are highly connected (degree) and influential (eigenvector) in one microbiome tend to maintain similar levels of connectivity in the other microbiome. Conversely, the correlation for betweenness centrality was not significant (Spearman $r = 0.30$, $p = 0.09$) (Fig. 3C), suggesting that the roles of species as connectors or bridges vary more between the two microbiomes compared to their roles as directly connected or influential nodes .

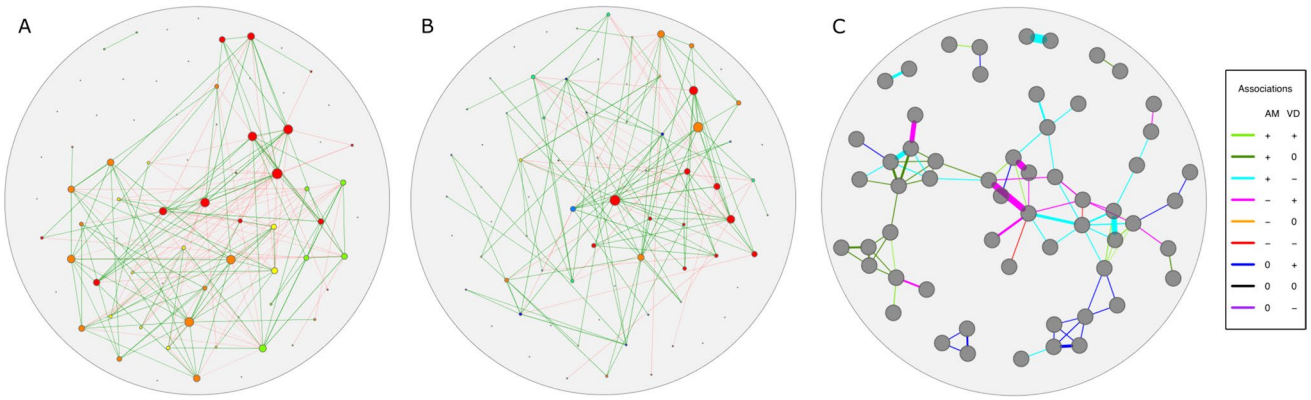

Fig. 2 Comparative network analysis. NetCoMi was applied to study the differences in the centrality of bacterial taxa and connectivity between them in the networks with the threshold value of SparCC ≥ 0.3 or ≤ −0.3, namely, *A. mellifera* (**A**), *V. destructor* (**B**), and differential network (**C**). Each node represents a single bacterial taxon, its size is proportional to eigenvector centrality, and its color is based on modularity class. Links determine relations between the nodes while their colors (in **A** and **B**)—red and green—mean positive and negative interactions, respectively. The colors of links (in **C**) are displayed in the legend of the figure and their edge width is directly proportional to the strength of the interaction. The symbols of plus (+), minus (−), and zero (0) correspond to positive, negative, and neutral associations, respectively

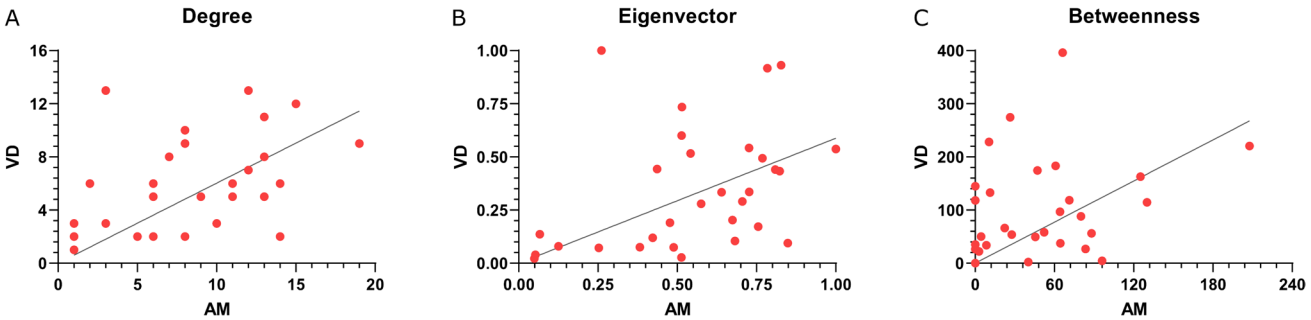

Fig. 3 Correlation across node centrality measures. Graphs represent the linear regression of taxa from the networks with a threshold value of SparCC ≥ 0.3 or ≤ −0.3. The topological features of degree (Spearman $r = 0.41$, $p = 0.02$) (**A**) and eigenvector (Spearman $r = 0.50$, $p = 0.004$) (**B**) centrality presented statistically significant results, while betweenness (**C**) did not (Spearman $r = 0.30$, $p = 0.09$) according to Spearman test. *X*- and *y*-axis correspond to *A. mellifera* and *V. destructor* species, respectively

The Jaccard index was used to assess the similarity in centrality distribution between the two networks under study. The findings indicated that the distribution for betweenness and closeness centrality metrics within networks at the lower threshold (SparCC ≥ 0.3 or ≤ −0.3) was higher than expected by random (Table 3), highlighting specific areas of alignment between the microbiome structures of honeybees and *Varroa* mites. At the higher interaction strength threshold (SparCC ≥ 0.5 or ≤ −0.5), all considered centrality measures were randomly distributed (Table 4).

When examining the top ten taxa with the highest centrality in terms of degree, eigenvector, and betweenness (SparCC ≥ 0.3 or ≤ −0.3) (Supplementary Table S1), six taxa were identified as common to both microbiomes (Supplementary Table S2). Upon applying the higher threshold for interactions (SparCC ≥ 0.5 or ≤ −0.5), among the top ten taxa (Supplementary Table S3), it was found the same number of shared taxa (Supplementary Table S4), but they were different from those found in the lower threshold.

Table 3 Jaccard index for honeybees and *Varroa* networks at a low threshold

Centrality measures	Jacc	*P* (≤Jacc)	*P* (≥Jacc)
Degree	0.422	0.92	0.13
Betweenness centrality	0.463	0.97	0.05*
Closeness centrality	0.489	0.99	0.01*
Eigenvector centrality	0.429	0.93	0.10
Hub taxa	0.411	0.93	0.10

Jaccard index for co-occurrence networks with the threshold of SparCC ≥ 0.3 or ≤ −0.3, * $p \leq 0.05$

Table 4 Jaccard index for honeybees and *Varroa* networks at a high threshold

Centrality measures	Jacc	P (≤Jacc)	P (≥Jacc)
Degree	0.429	0.89	0.19
Betweenness centrality	0.200	0.20	0.92
Closeness centrality	0.429	0.89	0.19
Eigenvector centrality	0.429	0.89	0.19
Hub taxa	0.429	0.89	0.19

Jaccard index for co-occurrence networks with the threshold of SparCC ≥ 0.5 or ≤ −0.5

Functional diversity and composition in *Varroa* mite and honeybee microbiomes

The predicted functional profiles of the microbiomes associated with honeybees and *Varroa* mites were analyzed to assess their potential metabolic capabilities. This analysis indicated a higher functional richness in the *Varroa* mite microbiome compared to the honeybee microbiome (Kruskal–Wallis test, $p < 0.01$, Fig. 4A). However, the analysis of mean Pielou's evenness, showed no statistical difference between the two microbiomes despite a numerical increase in the *Varroa* mite microbiome (Kruskal–Wallis test, $p > 0.05$, Fig. 4B). The Bray–Curtis dissimilarity index further revealed a significant difference in the functional profiles within the *Varroa* mite and honeybee microbiomes (PERMANOVA, $p = 0.000$), indicating a greater variation (ANOVA, $p = 0.000$) in the functional profiles among individual *Varroa* mites than among individual honeybees (Fig. 4C).

An examination of specific metabolic pathways identified differences in their relative abundance between the two microbiomes (Fig. 4D, Supplementary Table S5). A composition analysis further revealed both unique and shared metabolic pathways within the microbiomes of honeybees and *Varroa* mites (Fig. 4E). The honeybee microbiome was found to contain five unique enzymatic pathways, including glycolysis and uronate degradation, among others (Table 5). In contrast, the *Varroa* mite microbiome was characterized by ten unique pathways, such as vitamin E biosynthesis and sucrose degradation (Table 5). Despite these unique pathways, there was a substantial overlap, with 389 pathways

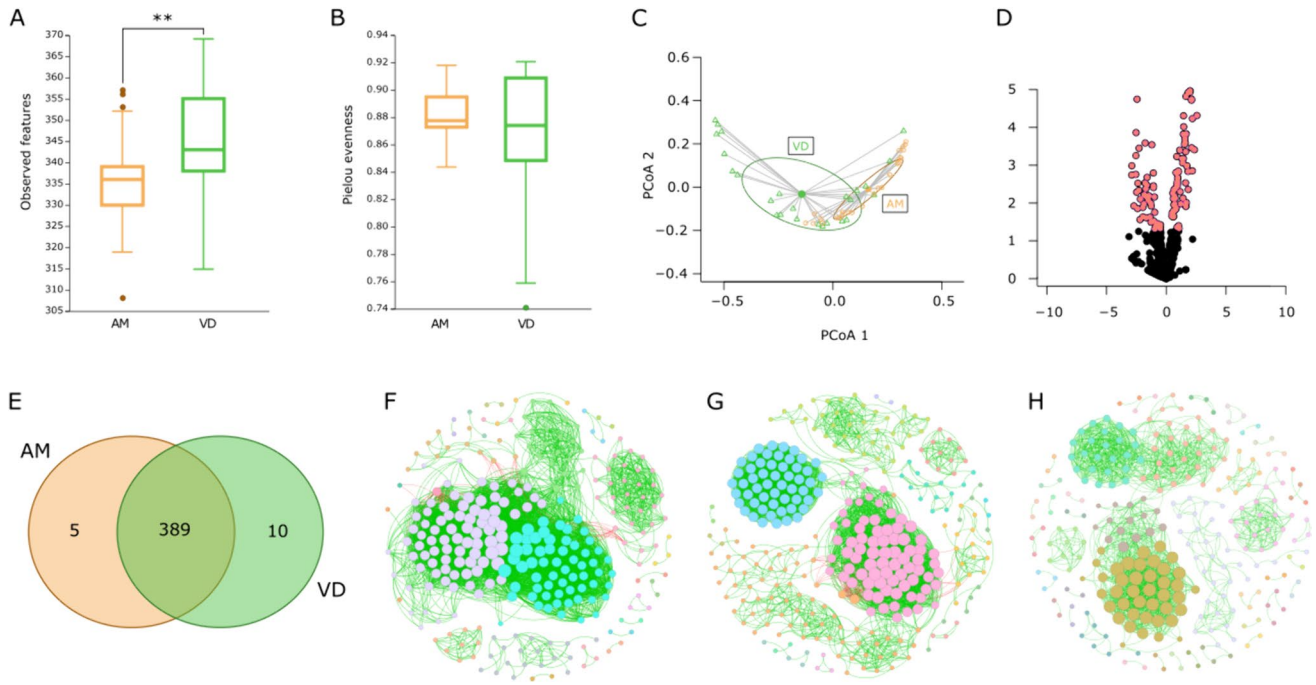

Fig. 4 Predicted functional profiles. Comparison of predicted functional profiles of *A. mellifera* and *V. destructor*. Observed features ($p = 0.004$) (**A**), Pielou's evenness ($p = 0.55$ (**B**), and Bray–Curtis distance ($p = 0.0001$, $F = 12.02$, stress 0.07488) (**C**) were applied to measure pathway diversity. Volcano plot (**D**) shows differential pathway abundance of *A. mellifera* and *V. destructor* microbiome. Pink color stands for significant differences among the groups. Venn diagram (**E**) displays shared and unique predicted bacterial pathways for both, *A. mellifera* and *V. destructor* microbiome. Co-occurrence networks of predicted pathways belonging to *A. mellifera* (**F**) and *V. destructor* (**G**) (SparCC ≥ 0.75 or ≤ −0.75). CAN analysis of honeybee and *Varroa* microbiomes (**H**). Nodes represent predicted enzymatic traits while their size and color are based on eigenvector centrality and modularity class, respectively. Red and green links stand for negative and positive interactions, respectively. Only the nodes with a minimum of one link are displayed

Table 5 Unique pathways in *Varroa* mites and honeybee microbiomes

Species	Pathways	
	Code	Name
AM[a]	P341-PWY	Glycolysis V (*Pyrococcus*)/archaeal EMP pathway
	PWY-6486	Uronic acid degradation/uronate degradation
	PWY-7031	Protein N-glycosylation (bacterial)
	PWY-7198	Pyrimidine deoxyribonucleotides de novo biosynthesis IV
	PWY-7210	Pyrimidine deoxyribonucleotides biosynthesis from CTP
VD[b]	PWY-1422	Vitamin E biosynthesis (tocopherols)
	PWY-3801	Sucrose degradation II (sucrose synthase)
	PWY-3941	Beta-alanine biosynthesis II
	PWY-5266	*p*-cymene degradation
	PWY-5273	*p*-cumate degradation
	PWY-5675	Nitrate assimilation
	PWY-6957	Mandelate degradation to acetyl-CoA
	PWY-7046	4-coumarate degradation (anaerobic)
	PWY-7084	Nitrous oxide biosynthesis/aerobic denitrification
	PWY5F9-12	Biphenyl degradation

[a]AM, *A. mellifera*

[b]VD, *V. destructor*

Table 6 Topological features of functional profile co-occurrence networks

Topology	AM75[a]	VD75[b]	CAN[c]
Average degree	39.261	25.745	12.222
Average weighted degree	33.093	21.849	11.062
Network diameter	10	14	9
Modularity	0.429	0.634	0.677
Average clustering coefficient	0.788	0.769	0.781
Nodes	284	314	261
Edges	5575	4042	1595
Positives	5490 (98.48%)	3960 (97.97%)	1595 (100%)
Negatives	85 (1.52%)	82 (2.03%)	0 (0%)

[a]*A. mellifera* (AM, network at threshold of SparCC ≥ 0.75 or ≤ -0.75 (AM75))

[b]*V. destructor* (VD, network at threshold of SparCC ≥ 0.75 or ≤ -0.75 (VD75))

[c]Core Association Network (CAN at threshold of SparCC ≥ 0.75 or ≤ -0.75 (CAN75))

shared between the two microbiomes (Supplementary Table S6).

Central pathways in functional networks of *Varroa* mite and honeybee microbiomes

The analysis of functional networks revealed distinct topological properties (Table 6) in the microbiomes of honeybees (Fig. 4F) and *Varroa* mites (Fig. 4G). Specifically, the honeybee microbiome's functional network demonstrated a higher average degree and weighted degree compared to that of the *Varroa* mite. Despite these differences, both networks shared a similar average clustering coefficient. Notably, the network associated with honeybees contained a greater number of edges, whereas the *V. destructor* network had a higher count of nodes (Table 6).

To identify the core pathway interaction between the two species, CAN analysis was conducted (Fig. 4H). This analysis showed that the functional profiles of the honeybee and *Varroa* mite had 261 nodes and 1595 edges in common, all characterized by positive interactions (Table 6). Central pathways within these functional networks were evaluated based on their centrality measures, including degree, eigenvector, and betweenness centrality. The analysis of the top third of pathways with the highest centrality revealed an overlapping rate of 63.22% for pathways ranking high in both degree and betweenness centrality and a notably higher overlap of 96.55% for pathways ranking high in both degree and eigenvector centrality.

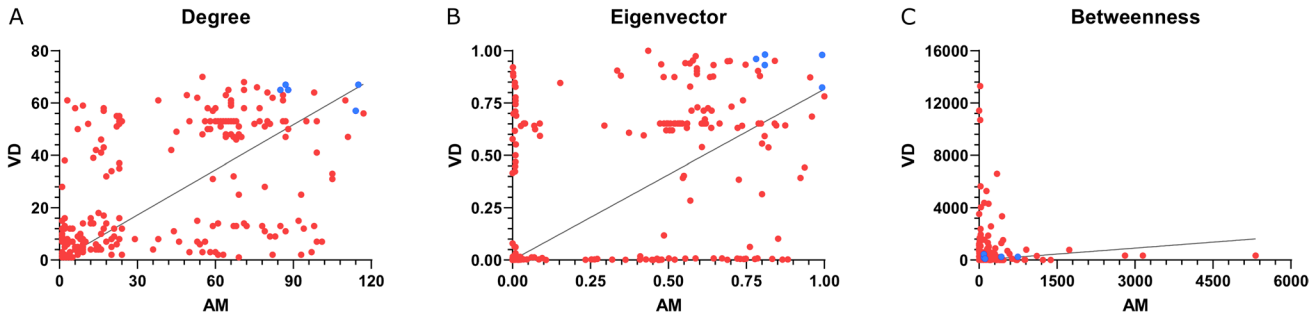

Fig. 5 Pathway correlation. Graphs show the linear regression of pathways from the networks with a threshold value of SparCC ≥ 0.75 or ≤ −0.75. Statistically significant results according to the Spearman test were presented in all topological features: degree (Spearman $r = 0.5679$, $p < 0.0001$) (**A**), eigenvector (Spearman $r = 0.5643$, $p < 0.0001$) (**B**), and betweenness (Spearman $r = 0.2325$, $p = 0.001$) (**C**). *X*- and *y*-axis correspond to *A. mellifera* and *V. destructor* species, respectively. The blue nodes represent five pathways that were selected for taxonomic contribution analysis and displayed in Sankey graphs

Table 7 Top pathways used for taxa contribution analysis

Code	Name
PWY-6125	Superpathway of guanosine nucleotides de novo biosynthesis II
PWY-6612	Superpathway of tetrahydrofolate biosynthesis/folic acid biosynthesis
PWY-7184	Pyrimidine deoxyribonucleotides de novo synthesis I
PWY-7539	6-hydroxymethyl-dihydropterin diphosphate biosynthesis III
FOLSYN-PWY	Superpathway of tetrahydrofolate biosynthesis and salvage

Correlation analysis of the pathways selected from the functional profile networks showed statistically significant associations across all measured topological features: degree (Spearman $r = 0.56$, $p = 0.0001$, Fig. 5A), eigenvector (Spearman $r = 0.56$, $p = 0.0001$, Fig. 5B), and betweenness (Spearman $r = 0.23$, $p = 0.0001$, Fig. 5C), highlighting the interconnectedness and functional significance of these pathways within the microbiomes.

Functional redundancy and niche differentiation in *Varroa* mite and honeybee microbiomes

Given the observed overlap in central pathways between the honeybee and *Varroa* mite microbiomes (Fig. 5), we hypothesized that these pathways represent core microbial processes essential for the survival and health of both organisms. The presence of these pathways in multiple taxa within each microbiome would indicate a broad functional redundancy, contributing to the microbiome's resilience and stability against environmental perturbations. Additionally, variations in the taxonomic contributions to these pathways could demonstrate how each microbiome is uniquely adapted to its respective host, indicating niche specialization.

To test this hypothesis, an analysis was conducted on the top five pathways (Fig. 6A) that exhibited the highest degree of centrality and were further supported by eigenvector centrality (Table 7). These pathways, primarily related to biosynthesis processes, were investigated for taxa contributions. Remarkably, a similar proportion of bacterial taxa, 22 out of 29 (75.86%) in honeybees and 21 out of 28 (75%) in *Varroa* mites, were found to be involved in these pathways .

Analysis of taxa contributions highlighted that both shared and unique bacterial taxa across the honeybee and *Varroa* mite microbiomes contributed to these pathways. Specifically, the analysis revealed 14 taxa unique to honeybees, 13 unique to *Varroa* mites, and 15 taxa shared between them, indicating a mixture of functional redundancy and taxonomic uniqueness (Fig. 6B, Supplementary Table S7). Notably, taxa such as *Morganella*, *Lactobacillus*, and others were identified as significant contributors to the pathways in both microbiomes, albeit with varying percentages (Fig. 6C).

Furthermore, the investigation into the most abundant bacterial taxa, as represented in a Sankey graph (Fig. 6A), confirmed their presence in both microbiomes under a SparCC threshold of ≥ 0.3 or ≤ −0.3 (Fig. 1AB). However, *Pseudomonas* was absent in *Varroa*. Only a select few taxa like *Lactobacillus* and *Snodgrassella* were present in the core taxonomic networks of both species (Fig. 1E). Differences in the topological measures of the nodes representing taxa driving the primary pathways were also observed (Table 8).

These results underline the existence of both functional redundancy and niche specialization within the microbiomes

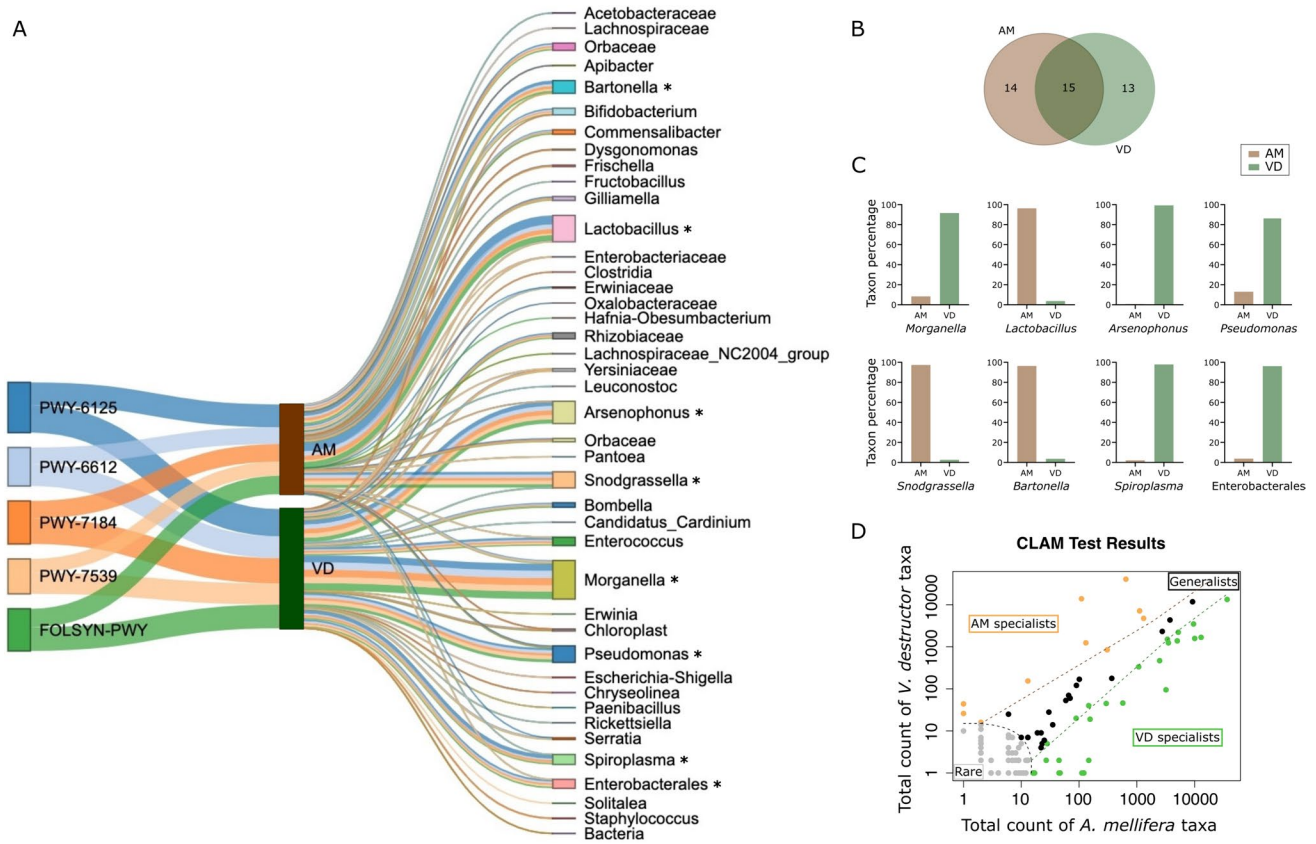

Fig. 6 Taxonomic contributions to metabolic pathways. In the Sankey graph (**A**), the columns on the left side represent selected pathways, the middle stands for species, and the last column on the right side corresponds to the names of bacterial taxa. The width of the lines is proportional to the value of taxon relative function abundance. Venn diagram (**B**) shows unique and shared bacterial taxa of the pathways that were selected for the Sankey graph. Eight graphs (**C**) represent the most abundant bacterial taxa (denoted by asterisks (*)) in the Sankey graph. The CLAM graph (**D**) represents taxa categorized as honeybee specialists (orange), *Varroa* specialists (green), generalists (black), and rare taxa (grey). In all, *A. mellifera* and *V. destructor* were abbreviated as AM and VD

Table 8 Contribution of bacterial taxa to the community assembly

	Degree			Eigenvector			Betweenness		
	AM[a]	VD[b]	CAN[c]	AM[a]	VD[b]	CAN[c]	AM[a]	VD[b]	CAN[c]
Morganella	8,00	9,00	–	0,51	0,73	–	47,09	174,39	–
Lactobacillus	11,00	6,00	0,91	0,76	0,17	–	130,03	114,38	4,00
Arsenophonus	13,00	5,00	–	0,77	0,49	–	96,03	4,39	–
Pseudomonas	13,00	–	–	0,77	–	–	116,01	–	–
Snodgrassella	13,00	11,00	1,59	0,82	0,43	–	66,16	396,04	0,00
Bartonella	7,00	8,00	–	0,54	0,52	–	11,21	132,95	–
Spiroplasma	14,00	2,00	–	0,85	0,09	–	88,02	56,00	–
Enterobacterales	9,00	5,00	0,51	0,48	0,19	–	80,09	88,25	5,00

[a] *A. mellifera* (AM, network at threshold of 0.3)

[b] *V. destructor* (VD, network at threshold of 0.3)

[c] Core Association Network (CAN at threshold of 0.3)

of honeybees and *Varroa* mites. A CLAM analysis further delineated the taxa according to their relative abundance into specialists for either honeybee or *Varroa*, generalists, and taxa considered too rare (Fig. 6D). This analysis found that specialists for honeybee comprised the smallest group, whereas *Varroa* mites had a larger group of specialists, alongside groups of generalists and a considerable number of taxa categorized as too rare (Supplementary Table S8).

Discussion

This study builds upon the work of Hubert et al. (2016), adding insights into the assembly of microbial communities of *Varroa* and honeybees. The significance of our paper lies in the comparison of the microbiomes of *A. mellifera* honeybees and *V. destructor* mites, in regard to their networks and potential functional profiles. It is noteworthy that only two studies exist delving into the comparison of the microbiomes of honeybees and *Varroa* mites, with contributions of Hubert et al. (2016) and Sandionigi et al. (2015). Belonging to the same taxonomic rank within the Arthropoda phylum, these two species share numerous common characteristics, suggesting a potentially shared microbial spectrum (Donovan and Paul 2005; Rosenkranz et al. 2010).

Our results indicate that the microbiome networks of *A. mellifera* are characterized by a higher number of bacterial nodes compared to those of *V. destructor*. Building on Hubert et al.'s (2016) explanation of lower bacterial diversity in *Varroa* mites resulting from the transfer of bacteria from honeybees to the mite body (rather than vice versa), we draw on the findings of Liu et al. (2023). Their research demonstrated a positive correlation between gut bacterial richness and the size of the stingless bee *Tetragonula carbonaria*, suggesting a proportional link between the body size of a model animal and its microbial richness. Applying this concept to our study, the bacterial diversity of *A. mellifera* is posited to be richer than that of *V. destructor* mites due to the larger body size of honeybees. However, the difference between the number of bacterial nodes is not significantly apparent; therefore, we suppose the similarity of both species may be induced by sharing the same environment of the beehive as the *Varroa* mites are associated with honeybees from the early stage of their life cycle. In contrast, our analysis of functional profiles reveals that the *V. destructor* microbiome encompasses a higher number of metabolic pathways compared to *A. mellifera*. This discrepancy could be attributed to the application of acaricidal treatments (formic acid or tau-fluvalinate) for 7 days, as noted by Hubert et al. (2016). Aligning with the findings of Kakumanu et al. (2016), who reported significant changes in the structure and functional profile of *A. mellifera* gut bacterial communities induced by pesticides, our findings highlight the potential impact of acaricidal treatment on microbiome characteristics. Moreover, the mites analyzed by Hubert et al. (2016) were collected from the bottom board of the hives after 7-day treatment, and as a consequence, the microbial community of the dead mites could differ from the microbial community of mites that were alive and present in the hive.

The robustness analysis of honeybee and *Varroa* mite microbiomes, focusing on their response to the addition and removal of nodes or taxa, sheds light on the intricate dynamics underpinning the resilience and functionality of these microbial communities. Higher LCC values suggest that both microbiomes are characterized by a high degree of interconnectedness, facilitating efficient resource and information flow and enhancing the ecosystem's resilience to environmental stressors through functional stability and redundancy. Conversely, higher APL values indicate a more compartmentalized or modular community structure, potentially offering resilience against localized disturbances by limiting their spread across the network. However, the differential impact observed during node removal, particularly the more significant effect on the *Varroa* microbiome and the distinct resilience patterns during targeted and cascading attacks, highlights nuanced differences in network structure and resilience strategies between the two microbiomes. Specifically, the honeybee microbiome exhibits greater resilience to targeted removals, suggesting a network better adapted to withstand losses of key species, whereas the *Varroa* microbiome demonstrates greater robustness to cascading failures, possibly indicating a different arrangement of essential functions. These insights emphasize the ecological significance of network structure in microbial communities, with implications for understanding ecosystem stability, managing microbial health, and conserving biodiversity.

Our analysis of predicted functional pathways suggests the existence of unique pathways in *Varroa* and honeybee microbiomes. For instance, pathways PWY-7198 and PWY-7210, found exclusively in *Apis* honeybees, are involved in the biosynthesis of pyrimidine, a crucial component of DNA and RNA (Sharma et al. 2014). Pyrimidines and their derivatives exhibit a wide range of biological activities, including antibacterial (Sharma et al. 2004), antifungal (Agarwal et al. 2000), antiviral (Balzarini 2002), and antiparasitic effects (Poletto et al. 2021). This suggests that honeybee bacteria might produce pyrimidine synthesis pathways to defend themselves against *Varroa* mites and/or the pathogens they transmit.

Additionally, other unique pathways in the honeybee, such as P341-PWY, PWY-6486, and PWY-7031, are related to energy production. This energy may be used to bolster the honeybee's immune system and protect the host organism. Conversely, *V. destructor* mites have unique pathways associated with the breakdown of various molecules, like sucrose and biphenyl, which help in energy release or metabolism, providing various benefits. For example, the degradation of sucrose produces glucose and fructose, crucial energy sources (Ruan 2014), while biphenyl breakdown leads to benzoate, a compound with toxic effects (Larson et al. 2021) such as acaricidal activity (Mostafiz et al. 2020). These processes could serve as defense mechanisms for mites against treatments or as part of the honeybee's immune response.

Furthermore, pathways in mites related to cumate degradation could influence gene expression and cell control (Seo and Schmidt-Dannert 2019; Klotz et al. 2023), while the synthesis of vitamin E and beta-alanine indicates potential anti-oxidant defensive strategies (Zingg 2019; Wang et al. 2021) against the oxidative machinery of the honeybee's immune system. Beta-alanine, a precursor for vitamin B5 and coenzyme A, is vital for cell formation and metabolism. It is interesting to note that plants produce beta-alanine in response to stress (Wang et al. 2021), suggesting mites might similarly use it to counteract acaricidal treatments or the effects of the honeybee immune system. This analysis underscores the complex interplay of biochemical pathways in host-parasite interactions and their potential roles in defense and survival.

We observed several instances of niche specialization in both *Varroa* and honeybee microbiomes. Numerous ecological and evolutionary theories highlight the diversity within ecological niches, pointing out the critical importance of niche diversification. This diversification process plays a pivotal role in shaping various ecological aspects (Bajić et al. 2021). Notably, it can result in niche specialization and differentiation, which enhances community stability by allowing multiple bacterial taxa to coexist (Kang et al. 2020). Each of these taxa contributes unique metabolic traits, supporting the community's overall function. When bacterial species show varied responses to environmental changes, this diversity can enhance community stability (Yachi and Loreau 1999). This adaptability is partly due to metabolic plasticity, allowing bacteria to adjust their metabolic processes in response to environmental shifts. Such adaptability is crucial for surviving global environmental changes (Malard and Guisan 2023), demonstrating how niche differentiation allows microbial communities to adapt and thrive under varying conditions. For example, high functional redundancy has been described in the gut microbiome of *Apis mellifera* and *Apis cerana*, even though both honeybee species harbor different bacterial strains and occupy different ecological niches (Wu et al. 2022). Our results can also be interpreted in light of the insurance hypothesis (Yachi and Loreau 1999), which posits that higher diversity can enhance ecosystem resilience to perturbations.

Several factors could influence the analysis of honeybee and *Varroa* microbiomes. Manipulation of both species may induce various changes, such as alterations in morphology or stress responses. Additionally, the choice of laboratory techniques (e.g., type of primers), their application (e.g., DNA isolation method), and the excision of organ tissues (e.g., whole body or gut) are critical considerations in the experimental design. The use of predicted metabolic pathways is also a limitation of this study. This kind of prediction could underestimate the actual pathway diversity as some genomes may not be available or are not incorporated in reference datasets with which this method works (Douglas et al. 2020). Importantly, the absence of a control sample raises concerns about potential sample contamination from surfaces, air, or isolation errors. Furthermore, the interactions between the honeybees themselves as well as with the environment are other agents impacting their microbiome composition. It is challenging to avoid these points as the honeybees are social animals, however, in future analyses, we recommend eluding acaricidal treatments before experiments and including control samples to account for potential contamination and minimize side effects in the analyses.

Conclusions

Our study on community assembly and network robustness in the *Varroa* and honeybee microbiomes provides valuable insights into the interplay between these two species and their associated bacterial communities. The co-occurrence network analyses, conducted at different thresholds, reveal topological features in *Varroa* and honeybee microbiomes, with honeybee networks generally exhibiting slightly higher values. However, the identification of shared core interactions suggests commonalities in microbial relationships between these two species. Furthermore, the differential networks and unique pathways observed in honeybee and *Varroa* microbiomes may reflect adaptations to their respective ecological niches, supporting the notion of niche specialization. The presence of shared pathways and bacterial taxa highlights potential functional redundancy in the metabolic capabilities of these microbial communities. Despite the slightly lower abundance of bacterial nodes in the mite microbiome, its greater richness in the functional profile implies that they may serve as an "insurance" reservoir of metabolic pathways, contributing to their resilience against environmental changes or stressors.

Supplementary Information The online version contains supplementary material available at https://doi.org/10.1007/s10123-024-00582-y.

Author contributions Štefánia Skičková: Conceptualization, Visualization, Formal analysis, Writing—Original Draft, Writing—Review & Editing; Myriam Kratou: Formal analysis, Writing—Original Draft; Karolína Svobodová: Writing—Original Draft; Apolline Maitre: Formal analysis, Data Curation, Writing—Review & Editing; Lianet Abuin-Denis: Formal analysis, Writing—Review & Editing; Alejandra Wu-Chuang: Supervision, Writing—Review & Editing; Dasiel Obregón: Methodology, Software, Writing—Review & Editing; Mourad Ben Said: Writing—Review & Editing; Viktória Majláthová: Writing—Review & Editing; Alena Krejčí: Writing—Review & Editing; Alejandro Cabezas-Cruz: Conceptualization, Visualization, Supervision, Writing—Original Draft, Writing—Review & Editing.

Funding Štefánia Skičková is supported by the Slovak Academic Information Agency via the National Scholarship Program of the Slovak Republic. Alejandra Wu-Chuang is supported by the Programa Nacional de Becas de Postgrado en el Exterior "Don Carlos Antonio

López" (grant no. 205/2018). Apolline Maitre is supported by the "Collectivité de Corse," grant: "Formations Superieures" (SGCE-RAPPORT no 0300). UMR BIPAR is supported by the French Government's Investissement d'Avenir program, Laboratoire d'Excellence "Integrative Biology of Emerging Infectious Diseases" (grant no. ANR-10-LABX-62-IBEID).

Data availability In the present study, we used available 16S rRNA amplicon sequence datasets. In the original study, Hubert et al. (2016) compared microbial diversity of A. mellifera honeybee and V. destructor mite within the hives. A 16S rRNA gene fragment was PCR amplified by barcoded primers 27Fmod/ill519Rmod and sequenced in Illumina TruSeq. Generated data were deposited in National Center for Biotechnology Information (NCBI) GenBank under the SRA number SRP067076.

Declarations

Ethics approval and consent to participate Not applicable.

Competing interests The authors declare no competing interests.

References

Aderem A (2005) Systems biology: its practice and challenges. Cell 121:511–513. https://doi.org/10.1016/j.cell.2005.04.020

Agarwal N, Raghuwanshi SK, Upadhyay DN, Shukla PK, Ram VJ (2000) Suitably functionalised pyrimidines as potential antimycotic agents. Bioorg Med Chem Lett 10:703–706. https://doi.org/10.1016/S0960-894X(00)00091-3

Allaire JJ, Gandrud C, Russell K, Yetman CJ, Ellis P, Kuo K, Lewis BW, Owen J, Rogers J, Sese C (2017) NetworkD3: D3 JavaScript Network Graphs from R (Version 0.4) [R package]. CRAN. https://CRAN.Rproject.org/package=networkD3

Anaconda Software Distribution (2023) Anaconda documentation. Anaconda Inc. https://Docs.Anaconda.Com.

Bajić D, Rebolleda-Gómez M, Muñoz MM, Sánchez Á (2021) The macroevolutionary consequences of niche construction in microbial metabolism. Front Microbiol 12:718082. https://doi.org/10.3389/fmicb.2021.718082

Balzarini J (2002) Bicyclic pyrimidine nucleoside analogues (BCNAs) as highly selective and potent inhibitors of varicella-zoster virus replication. J Antimicrob Chemother 50:5–9. https://doi.org/10.1093/jac/dkf037

Bastian M, Heymann S, Jacomy M (2009) Gephi: an open source software for exploring and manipulating networks. Proc Int AAAI Conf Web Soc Media 3:361–362. https://doi.org/10.1609/icwsm.v3i1.13937

Bokulich NA, Kaehler BD, Rideout JR, Dillon M, Bolyen E, Knight R, Huttley GA, Gregory Caporaso J (2018) Optimizing taxonomic classification of marker-gene amplicon sequences with QIIME 2's q2-feature-classifier plugin. Microbiome 6:90. https://doi.org/10.1186/s40168-018-0470-z

Bolyen E, Rideout JR, Dillon MR, Bokulich NA, Abnet CC, Al-Ghalith GA, Alexander H, Alm EJ, Arumugam M, Asnicar F, Bai Y, Bisanz JE, Bittinger K, Brejnrod A, Brislawn CJ, Brown CT, Callahan BJ, Caraballo-Rodríguez AM, Chase J, Cope EK, Da Silva R, Diener C, Dorrestein PC, Douglas GM, Durall DM, Duvallet C, Edwardson CF, Ernst M, Estaki M, Fouquier J, Gauglitz JM, Gibbons SM, Gibson DL, Gonzalez A, Gorlick K, Guo J, Hillmann B, Holmes S, Holste H, Huttenhower C, Huttley GA, Janssen S, Jarmusch AK, Jiang L, Kaehler BD, Kang KB, Keefe CR, Keim P, Kelley ST, Knights D, Koester I, Kosciolek T, Kreps J, Langille MGI, Lee J, Ley R, Liu Y-X, Loftfield E, Lozupone C, Maher M, Marotz C, Martin BD, McDonald D, McIver LJ, Melnik AV, Metcalf JL, Morgan SC, Morton JT, Naimey AT, Navas-Molina JA, Nothias LF, Orchanian SB, Pearson T, Peoples SL, Petras D, Preuss ML, Pruesse E, Rasmussen LB, Rivers A, Robeson MS, Rosenthal P, Segata N, Shaffer M, Shiffer A, Sinha R, Song SJ, Spear JR, Swafford AD, Thompson LR, Torres PJ, Trinh P, Tripathi A, Turnbaugh PJ, Ul-Hasan S, Van Der Hooft JJJ, Vargas F, Vázquez-Baeza Y, Vogtmann E, Von Hippel M, Walters W, Wan Y, Wang M, Warren J, Weber KC, Williamson CHD, Willis AD, Xu ZZ, Zaneveld JR, Zhang Y, Zhu Q, Knight R, Caporaso JG (2019) Reproducible, interactive, scalable and extensible microbiome data science using QIIME 2. Nat Biotechnol 37:852–857. https://doi.org/10.1038/s41587-019-0209-9

Callahan BJ, McMurdie PJ, Rosen MJ, Han AW, Johnson AJA, Holmes SP (2016) DADA2: High-resolution sample inference from Illumina amplicon data. Nat Methods 13:581–583. https://doi.org/10.1038/nmeth.3869

Caspi R, Billington R, Fulcher CA, Keseler IM, Kothari A, Krummenacker M, Latendresse M, Midford PE, Ong Q, Ong WK, Paley S, Subhraveti P, Karp PD (2018) The MetaCyc database of metabolic pathways and enzymes. Nucleic Acids Res 46:D633–D639. https://doi.org/10.1093/nar/gkx935

Chazdon RL, Chao A, Colwell RK, Lin S-Y, Norden N, Letcher SG, Clark DB, Finegan B, Arroyo JP (2011) A novel statistical method for classifying habitat generalists and specialists. Ecol 92:1332–1343. https://doi.org/10.1890/10-1345.1

Chen Y, Pettis JS, Evans JD, Kramer M, Feldlaufer MF (2004) Transmission of Kashmir bee virus by the ectoparasitic mite *Varroa destructor*. Apidologie 35:441–448. https://doi.org/10.1051/apido:2004031

DeSantis TZ, Hugenholtz P, Larsen N, Rojas M, Brodie EL, Keller K, Huber T, Dalevi D, Hu P, Andersen GL (2006) Greengenes, a chimera-checked 16S rRNA gene database and workbench compatible with ARB. App Environ Microbiol 72:5069–5072. https://doi.org/10.1128/AEM.03006-05

Di Prisco G, Pennacchio F, Caprio E, Boncristiani HF, Evans JD, Chen Y (2011) *Varroa destructor* is an effective vector of Israeli acute paralysis virus in the honeybee *Apis mellifera*. J Gen Virol 92:151–155. https://doi.org/10.1099/vir.0.023853-0

Donovan BJ, Paul F (2005) Pseudoscorpions: the forgotten beneficials inside beehives and their potential for management for control of *Varroa* and other arthropod pests. Bee World 86:83–87. https://doi.org/10.1080/0005772X.2005.11417322

Douglas GM, Maffei VJ, Zaneveld JR, Yurgel SN, Brown JR, Taylor CM, Huttenhower C, Langille MGI (2020) PICRUSt2 for prediction of metagenome functions. Nat Biotechnol 38:685–688. https://doi.org/10.1038/s41587-020-0548-6

Faust K, Raes J (2012) Microbial interactions: from networks to models. Nat Rev Microbiol 10:538–550. https://doi.org/10.1038/nrmicro2832

Fischhoff IR, Huang T, Hamilton SK, Han BA, LaDeau SL, Ostfeld RS, Rosi EJ, & Solomon CT (2020). Parasite and pathogen effects on ecosystem processes: a quantitative review. *Ecosphere*, *11*(5). https://doi.org/10.1002/ecs2.3057

Freitas S, Yang D, Kumar S, Tong H, Chau DH (2021) Evaluating graph vulnerability and robustness using TIGER. In 'Proc. 30th ACM Int. Conf. Inf. Knowl. Manag.', virtual event Queensland Australia. 4495–4503. (ACM: virtual event Queensland Australia) https://doi.org/10.1145/3459637.3482002.

Friedman J, Alm EJ (2012) Inferring correlation networks from genomic survey data (C Von Mering, Ed.). PLoS Comput Biol 8, e1002687. https://doi.org/10.1371/journal.pcbi.1002687.

Gliński Z, & Jarosz J (1992). *Varroa* jacobsoni as a carrier of bacterial infections to a recipient bee host. Apidologie 23(1):25–31. https://doi.org/10.1051/apido:19920103

Han B, Wu J, Wei Q, Liu F, Cui L, Rueppell O, Xu S (2024) Life-history stage determines the diet of ectoparasitic mites on their honey bee hosts. Nat Commun 25;15(1):725. https://doi.org/10.1038/s41467-024-44915-x

Hammer O, Harper D, Ryan P (2001) PAST: paleontological statistics software package for education and data analysis. Palaeontologia electronica 1–9.

Hou Y, Zhang X, Zhou Q, Hong W, Wang Y (2021) Hierarchical microbial functions prediction by graph aggregated embedding. Front Genet 11:608512. https://doi.org/10.3389/fgene.2020.608512

Hristov P, Shumkova R, Palova N, Neov B (2020) Factors associated with honey bee colony losses: a mini-review. Vet Sci 7:166. https://doi.org/10.3390/vetsci7040166

Huang Q, Evans JD (2024) Host switch by honey bee parasitic mites leads to symbiont diversification. J Invertebr Pathol 203:108068. https://doi.org/10.1016/j.jip.2024.108068

Hubert J, Bicianova M, Ledvinka O, Kamler M, Lester PJ, Nesvorna M, Kopecky J, Erban T (2017) Changes in the bacteriome of honey bees associated with the parasite *Varroa destructor*, and pathogens *Nosema* and *Lotmaria passim*. Microb Ecol 73:685–698. https://doi.org/10.1007/s00248-016-0869-7

Hubert J, Kamler M, Nesvorna M, Ledvinka O, Kopecky J, Erban T (2016) Comparison of *Varroa destructor* and worker honeybee microbiota within hives indicates shared bacteria. Microb Ecol 72:448–459. https://doi.org/10.1007/s00248-016-0776-y

Kakumanu ML, Reeves AM, Anderson TD, Rodrigues RR, Williams MA (2016) Honey bee gut microbiome is altered by in-hive pesticide exposures. Front Microbiol 7:1255. https://doi.org/10.3389/fmicb.2016.01255

Kanbar G, Engels W (2003) Ultrastructure and bacterial infection of wounds in honey bee (*Apis mellifera*) pupae punctured by *Varroa* mites. Parasitol Res 90:349–354. https://doi.org/10.1007/s00436-003-0827-4

Kanehisa M (2000) KEGG: Kyoto encyclopedia of genes and genomes. Nucleic Acids Res 28:27–30. https://doi.org/10.1093/nar/28.1.27

Kang S, Niu J, Zhang Q, Zhang X, Han G, Zhao M (2020) Niche differentiation is the underlying mechanism maintaining the relationship between community diversity and stability under grazing pressure. Glob Ecol Conserv 24:e01246. https://doi.org/10.1016/j.gecco.2020.e01246

Klotz A, Kaczmarczyk A, Jenal U (2023) A synthetic cumate-inducible promoter for graded and homogenous gene expression in *Pseudomonas aeruginosa* (PI Nikel, Ed.). App Environ Microbiol 89:e00211-e223. https://doi.org/10.1128/aem.00211-23

Kralj J, Fuchs S (2006) Parasitic *Varroa* destructor mites influence flight duration and homing ability of infested Apis mellifera foragers. Apidologie 37(5):577–587. https://doi.org/10.1051/apido:2006040

Kuster RD, Boncristiani HF, Rueppell O (2014) Immunogene and viral transcript dynamics during parasitic *Varroa* destructor mite infection of developing honey bee (Apis mellifera) pupae. J Exp Biol 217(10):1710–1718. https://doi.org/10.1242/jeb.097766

Larson NR, Nega M, Zhang A, Feldlaufer M (2021) Toxicity of methyl benzoate and analogs to adult Aedes aegypti. J Am Mosq Control Assoc 37:83–86. https://doi.org/10.2987/19-6896.1

Layeghifard M, Hwang DM, Guttman DS (2017) Disentangling interactions in the microbiome: a network perspective. Trends Microbiol 25:217–228. https://doi.org/10.1016/j.tim.2016.11.008

Lhomme S (2015) Analyse spatiale de la structure des réseaux techniques dans un contexte de risques. Cybergeo. https://doi.org/10.4000/cybergeo.26763

Liu H, Hall MA, Brettell LE, Wang J, Halcroft M, Nacko S, Spooner-Hart R, Cook JM, Riegler M, Singh BK (2023) Microbial diversity in stingless bee gut is linked to host wing size and influenced by the environment. J Invertebr Pathol 198:107909. https://doi.org/10.1016/j.jip.2023.107909

Love MI, Huber W, Anders S (2014) Moderated estimation of fold change and dispersion for RNA-seq data with DESeq2. Genome Biol 15:550. https://doi.org/10.1186/s13059-014-0550-8

Malard LA, Guisan A (2023) Into the microbial niche. Trends Ecol Evol 38:936–945. https://doi.org/10.1016/j.tree.2023.04.015

Mostafiz MM, Shim J, Hwang H, Bunch H, Lee K (2020) Acaricidal effects of methyl benzoate against *Tetranychus urticae* Koch (Acari: Tetranychidae) on common crop plants. Pest Manag Sci 76:2347–2354. https://doi.org/10.1002/ps.5770

Oksanen J, Simpson G, Blanchet FG, Kindt R, Legendre P, Minchin P, O'Hara RB, Solymos P, Stevens MHH, Szoecs E, Wagner H, Barbour M, Bedward M, Bolker B, Borcard D, Carvalho G, Chirico M, De Caceres M, Durand S, Evangelista HBA, FitzJohn R, Friendly M, Furneaux B, Hannigan G, Hill MO, Lahti L, McGlinn D, Ouellette M-H, Cunha ER, Smith T, Stier A, Braak CJFT, Weedon J (2022) vegan: Community Ecology Package (Version 2.6-6) [R package]. CRAN. https://github.com/vegandevs/vegan

Pakwan C, Kaltenpoth M, Weiss B, Chantawannakul P, Jun G, Disayathanoowat T (2018) Bacterial communities associated with the ectoparasitic mites *Varroa destructor* and *Tropilaelaps mercedesae* of the honey bee (*Apis mellifera*). FEMS Microbiol Ecol 93(12). https://doi.org/10.1093/femsec/fix160.

Peschel S, Müller CL, Von Mutius E, Boulesteix A-L, Depner M (2021) NetCoMi: network construction and comparison for microbiome data in R. Brief Bioinform 22(4):bbaa290. https://doi.org/10.1093/bib/bbaa290

Pielou EC (1966) The measurement of diversity in different types of biological collections. J Theor Biol 13:131–144. https://doi.org/10.1016/0022-5193(66)90013-0

Piou V, Schurr F, Dubois E, Vétillard A (2022) Transmission of deformed wing virus between *Varroa destructor* foundresses, mite offspring and infested honey bees. Parasit Vectors 15:333. https://doi.org/10.1186/s13071-022-05463-9

Poletto J, Da Silva MJV, Jacomini AP, Bidóia DL, Volpato H, Nakamura CV, Rosa FA (2021) Antiparasitic activities of novel pyrimidine N-acylhydrazone hybrids. Drug Dev Res 82:230–240. https://doi.org/10.1002/ddr.21745

Ramsey SD, Ochoa R, Bauchan G, Gulbronson C, Mowery JD, Cohen A, Lim D, Joklik J, Cicero JM, Ellis JD, Hawthorne D, vanEngelsdorp D (2019) *Varroa destructor* feeds primarily on honey bee fat body tissue and not hemolymph. Proc Nat Acad Sci 116:1792–1801. https://doi.org/10.1073/pnas.1818371116

Raymann K, Coon KL, Shaffer Z, Salisbury S, Moran NA, McFall-Ngai MJ (2018) Pathogenicity of Serratia marcescens strains in honey bees. Mbio 9(5):e01649-e1718. https://doi.org/10.1128/mBio.01649-18

Rosenkranz P, Aumeier P, Ziegelmann B (2010) Biology and control of *Varroa destructor*. J Invertebr Pathol 103:S96–S119. https://doi.org/10.1016/j.jip.2009.07.016

Röttjers L, Faust K (2018) From hairballs to hypotheses–biological insights from microbial networks. FEMS Microbiol Rev 42:761–780. https://doi.org/10.1093/femsre/fuy030

Röttjers L, Vandeputte D, Raes J, Faust K (2021) Null-model-based network comparison reveals core associations. ISME Communications 1:36. https://doi.org/10.1038/s43705-021-00036-w

RStudio Team (2020) RStudio: integrated development for RStudio, PBC, Boston, MA, USA. https://www.rstudio.com/

Ruan Y-L (2014) Sucrose metabolism: gateway to diverse carbon use and sugar signaling. Annu Rev Plant Biol 65:33–67. https://doi.org/10.1146/annurev-arplant-050213-040251

Ruano MV, Fernandez FM, Ochoa AC (1991) Varroasis disturbs the orientation of bees: Its influence on parasitosis development. Vida Apícola 3:55–57

Sandionigi A, Vicario S, Prosdocimi EM, Galimberti A, Ferri E, Bruno A, Balech B, Mezzasalma V, Casiraghi M (2015) Towards a better understanding of *Apis mellifera* and *Varroa destructor*

microbiomes: introducing 'PHYLOH' as a novel phylogenetic diversity analysis tool. Mol Ecol Res 15:697–710. https://doi.org/10.1111/1755-0998.12341

Seo S-O, Schmidt-Dannert C (2019) Development of a synthetic cumate-inducible gene expression system for *Bacillus*. App Microbiol Biotechnol 103:303–313. https://doi.org/10.1007/s00253-018-9485-4

Sharma P, Rane N, Gurram VK (2004) Synthesis and QSAR studies of pyrimido[4,5-d]pyrimidine-2,5-dione derivatives as potential antimicrobial agents. Bioorg Med Chem Lett 14:4185–4190. https://doi.org/10.1016/j.bmcl.2004.06.014

Sharma V, Chitranshi N, Agarwal AK (2014) Significance and biological importance of pyrimidine in the microbial world. Internat J Med Chem 2014:1–31. https://doi.org/10.1155/2014/202784

Su X (2021) Elucidating the beta-diversity of the microbiome: from global alignment to local alignment. mSystems 6:e00363-e421. https://doi.org/10.1128/mSystems.00363-21

Svobodová K, Maitre A, Obregón D, Wu-Chuang A, Thaduri S, Locke B, De Miranda JR, Mateos-Hernández L, Krejčí AB, Cabezas-Cruz A (2023) Gut microbiota assembly of Gotland *varroa*-surviving honey bees excludes major viral pathogens. Microbiol Res 274:127418. https://doi.org/10.1016/j.micres.2023.127418

Tantillo G, Bottaro M, Di Pinto A, Martella V, Di Pinto P, Terio V (2015) Virus infections of honeybees *Apis mellifera*. Ital J Food Safety 4(3):157–168. https://doi.org/10.4081/ijfs.2015.5364

Traynor KS, Mondet F, De Miranda JR, Techer M, Kowallik V, Oddie MAY, Chantawannakul P, McAfee A (2020) *Varroa destructor*: a complex parasite, crippling honey bees worldwide. Trends Parasitol 36:592–606. https://doi.org/10.1016/j.pt.2020.04.004

Vaidyanathan R, Xie Y, Allaire J, Cheng J, Sievert C, Russell K (2023) Htmlwidgets: HTML widgets for R (Version 1.6.4) [R package]. CRAN. https://github.com/ramnathv/htmlwidgets.

Wang L, Mao Y, Wang Z, Ma H, Chen T (2021) Advances in biotechnological production of β-alanine. World J Microbiol and Biotechnol 37:79. https://doi.org/10.1007/s11274-021-03042-1

Yachi S, Loreau M (1999) Biodiversity and ecosystem productivity in a fluctuating environment: the insurance hypothesis. Proc Nat Acad Sci 96:1463–1468. https://doi.org/10.1073/pnas.96.4.1463

Yarza P, Yilmaz P, Pruesse E, Glöckner FO, Ludwig W, Schleifer K-H, Whitman WB, Euzéby J, Amann R, Rosselló-Móra R (2014) Uniting the classification of cultured and uncultured bacteria and archaea using 16S rRNA gene sequences. Nat Rev Microbiol 12:635–645. https://doi.org/10.1038/nrmicro3330

Ziemski M, Adamov A, Kim L, Flörl L, Bokulich NA (2022) Reproducible acquisition, management and meta-analysis of nucleotide sequence (meta)data using q2-fondue (J Wren, Ed.). Bioinform 38:5081–5091. https://doi.org/10.1093/bioinformatics/btac639

Zingg J (2019) Vitamin E: regulatory role on signal transduction. IUBMB Life 71:456–478. https://doi.org/10.1002/iub.1986

Terms and Conditions

Springer Nature journal content, brought to you courtesy of Springer Nature Customer Service Center GmbH (“Springer Nature”).
Springer Nature supports a reasonable amount of sharing of research papers by authors, subscribers and authorised users (“Users”), for small-scale personal, non-commercial use provided that all copyright, trade and service marks and other proprietary notices are maintained. By accessing, sharing, receiving or otherwise using the Springer Nature journal content you agree to these terms of use (“Terms”). For these purposes, Springer Nature considers academic use (by researchers and students) to be non-commercial.
These Terms are supplementary and will apply in addition to any applicable website terms and conditions, a relevant site licence or a personal subscription. These Terms will prevail over any conflict or ambiguity with regards to the relevant terms, a site licence or a personal subscription (to the extent of the conflict or ambiguity only). For Creative Commons-licensed articles, the terms of the Creative Commons license used will apply.
We collect and use personal data to provide access to the Springer Nature journal content. We may also use these personal data internally within ResearchGate and Springer Nature and as agreed share it, in an anonymised way, for purposes of tracking, analysis and reporting. We will not otherwise disclose your personal data outside the ResearchGate or the Springer Nature group of companies unless we have your permission as detailed in the Privacy Policy.
While Users may use the Springer Nature journal content for small scale, personal non-commercial use, it is important to note that Users may not:

1. use such content for the purpose of providing other users with access on a regular or large scale basis or as a means to circumvent access control;
2. use such content where to do so would be considered a criminal or statutory offence in any jurisdiction, or gives rise to civil liability, or is otherwise unlawful;
3. falsely or misleadingly imply or suggest endorsement, approval , sponsorship, or association unless explicitly agreed to by Springer Nature in writing;
4. use bots or other automated methods to access the content or redirect messages
5. override any security feature or exclusionary protocol; or
6. share the content in order to create substitute for Springer Nature products or services or a systematic database of Springer Nature journal content.

In line with the restriction against commercial use, Springer Nature does not permit the creation of a product or service that creates revenue, royalties, rent or income from our content or its inclusion as part of a paid for service or for other commercial gain. Springer Nature journal content cannot be used for inter-library loans and librarians may not upload Springer Nature journal content on a large scale into their, or any other, institutional repository.
These terms of use are reviewed regularly and may be amended at any time. Springer Nature is not obligated to publish any information or content on this website and may remove it or features or functionality at our sole discretion, at any time with or without notice. Springer Nature may revoke this licence to you at any time and remove access to any copies of the Springer Nature journal content which have been saved.
To the fullest extent permitted by law, Springer Nature makes no warranties, representations or guarantees to Users, either express or implied with respect to the Springer nature journal content and all parties disclaim and waive any implied warranties or warranties imposed by law, including merchantability or fitness for any particular purpose.
Please note that these rights do not automatically extend to content, data or other material published by Springer Nature that may be licensed from third parties.
If you would like to use or distribute our Springer Nature journal content to a wider audience or on a regular basis or in any other manner not expressly permitted by these Terms, please contact Springer Nature at

onlineservice@springernature.com